

# Hydraulics of a finite-diameter horizontal well with wellbore storage and skin effect

Eungyu Park <sup>\*</sup>, Hongbin Zhan

*Department of Geology and Geophysics, Texas A&M University, College Station, TX 77843-3115, USA*

Received 23 July 2001; received in revised form 14 January 2002; accepted 30 January 2002

## Abstract

We have obtained solutions of groundwater flow to a finite-diameter horizontal well including wellbore storage and skin effect in a three-dimensionally anisotropic leaky aquifer. These solutions improve previous line source solutions by considering realistic well geometry and offer better description of drawdown near the horizontal well. These solutions are derived on the basis of the separation of the source and the geometric functions. The source function is analyzed using Laplace transformation, and the geometric function is derived based on the method of superposition. The solution in a confined aquifer is derived as a special case of the solution in a leaky aquifer. The graphically integrated computer program FINHOW is written to generate type curves of groundwater flow to a finite-diameter horizontal well. The influence of the finite-diameter of the well, the wellbore storage, the skin effect, the leakage parameter, and the aquifer anisotropy is thoroughly analyzed. The well diameter, the wellbore storage, the skin effect, and the aquifer anisotropy substantially affect the near-well early time drawdown if compared to the line source solution, but they have negligible influence upon the far field or late time drawdown. This research provides a better tool for interpreting finite-diameter horizontal well pumping tests. © 2002 Elsevier Science Ltd. All rights reserved.

## 1. Introduction

Horizontal wells have screen sections parallel to the horizontal directions. These wells have been widely used in petroleum engineering [21,26,44], and agricultural and civil engineering [15,31] in the past. They have gained significant interests among hydrogeologists, environmental scientists, and engineers in recent years [11,18,43,50–52]. Horizontal wells have advantages that are irreplaceable by vertical wells at some circumstances. For instance, they can be used at sites where ground surfaces are obstructed by permanent structures such as buildings, highways, railways, wetlands, landfills, etc.; they can have great contact areas with the thin ground water aquifers; they can be effective in recovering thin layer contaminants; they can perform better recovery in vertically fractured aquifers, etc.

Hantush and Papadopoulos [15] have initially investigated the hydraulics of a collector well, which is a series of horizontal wells distributed in a horizontal plane. Petroleum engineers have studied fluid flow to hori-

zontal wells in oil and gas reservoirs [7,12,42]. In recent years, hydrogeologists have studied hydraulics of horizontal wells in shallow ground water aquifers [5,43,50–52]. In most of these studies, the horizontal well is treated as a line source and the well storage and skin effect are not included. The wellbore storage refers to water initially stored inside the well; the skin effect refers to the alteration of hydraulic conductivity at a thin layer immediately outside the wellbore during the well-installation process. The well skin serves as a barrier separating the wellbore from the aquifer.

Extensive studies on hydraulics of finite or large diameter vertical wells, including the wellbore storage and skin effect, have been reported before [3,4,9,10,22,27,28,30,34,36,49]. The analytical solution for the drawdown produced by a large-diameter vertical well including fluid storage capacity was first presented by Van Everdingen and Hurst [48] in petroleum, and by Papadopoulos and Cooper [36] in groundwater literature. Those studies have been extensively applied to oil and gas well problems later [1,19,38–40,47]. Large diameter wells have been used for hydrological applications in homogeneous aquifers [20,27,28,36] and in heterogeneous aquifers [17]. They have been applied in confined aquifers [36,45], leaky aquifers [25,27], and water table aquifers [28].

<sup>\*</sup> Corresponding author. Tel.: +1-979-845-9683; fax: +1-979-845-6162.

E-mail address: park@hydrog.tamu.edu (E. Park).

### Nomenclature

$B_D$	dimensionless leakage coefficient	$q_f$	aquifer pumping rate ( $\text{m}^3/\text{s}$ )
$C_s$	conductance of wellbore skin ( $\text{s}^{-1}$ )	$q_{fD}$	dimensionless aquifer pumping rate
$d$	thickness of leaky confined aquifer (m)	$\bar{q}'_{fD}$	modified dimensionless aquifer pumping rate in Laplace domain
$d'$	thickness of leaky confining layer (m)	$q'_{fD}$	modified dimensionless aquifer pumping rate in real time domain
$d_s$	thickness of skin (m)	$r_c$	radius of the casing connected with the horizontal well screen (m)
$f$	averaged drawdown outside of the skin (m)	$r_D$	dimensionless horizontal distance from point source to monitoring location
$f_D$	dimensionless averaged drawdown outside of the skin	$r_s$	$= r_w + d_s$ , outer radius of the skin (m)
$\bar{f}_D$	dimensionless averaged drawdown outside of the skin in Laplace domain	$r_w$	wellbore radius (m)
$g_0$	dimensionless point geometric function	$r_{wD}$	dimensionless wellbore radius
$\bar{g}$	dimensionless geometric function of horizontal well in Laplace domain	$S_s$	specific storativity ( $\text{m}^{-1}$ )
$\bar{g}_0$	dimensionless point geometric function in Laplace domain	$s$	drawdown outside wellbore (m)
$\bar{g}^*$	dimensionless averaged geometric function of horizontal well in Laplace domain	$s_D$	dimensionless drawdown outside wellbore
$h$	hydraulic head (m)	$s_{HD}$	dimensionless drawdown caused by a horizontal well
$h_0$	initial hydraulic head (m)	$s'_D$	modified dimensionless drawdown outside wellbore
$K$	hydraulic conductivity of an isotropic aquifer ( $\text{m/s}$ )	$\bar{s}'_D$	modified dimensionless drawdown outside wellbore in Laplace domain
$K'$	hydraulic conductivity of leaky confining layer ( $\text{m/s}$ )	$s_w$	drawdown inside wellbore (m)
$K_0(\cdot)$	second kind zero-order modified Bessel function	$s_{wD}$	dimensionless drawdown inside wellbore
$K_s$	hydraulic conductivity of skin zone ( $\text{m/s}$ )	$t$	time (s)
$K_x, K_y, K_z$	principal hydraulic conductivities along $x$ -, $y$ -, and $z$ -axis, respectively ( $\text{m/s}$ )	$t_D$	dimensionless time
$L$	screen length of horizontal wellbore (m)	$V$	volume of finite diameter horizontal wellbore ( $\text{m}^3$ )
$L_D$	dimensionless screen length of horizontal wellbore	$x, y, z$	longitudinal, transversal, and vertical coordinates, respectively (m)
$L^{-1}(\cdot)$	inverse Laplace transform, respectively	$x_0, y_0, z_0$	coordinates of the point source along the $x$ -, $y$ -, and $z$ -axis (m)
$p$	Laplace transform variable with respect to dimensionless time	$x_{0D}, y_{0D}, z_{0D}$	dimensionless coordinates of the point source along the $x$ -, $y$ -, and $z$ -axis
$Q$	total pumping rate ( $\text{m}^3/\text{s}$ )	$x_D, y_D, z_D$	dimensionless coordinates of the monitoring point along the $x$ -, $y$ -, and $z$ -axis
$Q_f$	total aquifer pumping rate ( $\text{m}^3/\text{s}$ )	$z_w$	depth from the central axis of the horizontal well to the lower boundary (m)
$Q_w$	total wellbore storage pumping rate ( $\text{m}^3/\text{s}$ )	$\alpha$	dimensionless skin conductance coefficient
$Q_{fD}$	dimensionless total aquifer pumping rate	$\beta$	dimensionless wellbore storage coefficient
$Q_{wD}$	dimensionless total wellbore storage pumping rate	$\delta(\cdot)$	Dirac delta function
$\bar{Q}_{fD}$	dimensionless total wellbore storage pumping rate in Laplace domain	$\eta$	skin effect parameter
$q$	reference pumping rate ( $\text{m}^3/\text{s}$ )		

They have also been used to study problems with non-Darcian fluid flow [38,45].

However, hydraulics of a finite-diameter horizontal well, including the wellbore storage and skin effect, has rarely been studied before. The available references in this field include an analytical study for horizontal wells with wellbore storage and skin in a layered petroleum

reservoir [24]; and an analysis of horizontal wells in a bounded naturally fractured reservoir [33]. But those analytical studies only reflect the measurement of drawdown inside the wellbore based on the previous study on wellbore storage and skin effect [48]. Solutions for monitoring piezometers or wells were not available from those studies. Those solutions did not explicitly consider

the finite diameter of the horizontal wellbore, and they were not suitable for studying leaky confined aquifers.

It is the purpose of this paper to study hydraulics of horizontal wells under a more realistic circumstance, i.e., considering the actual diameter of a horizontal well and including the effect of the wellbore storage and the skin effect. The results derived in this paper will be closer to the physical reality of the horizontal well performance. These results will be compared with previous line source solutions to assess the sensitivity of ground water flow on the horizontal well diameter, the wellbore storage, the skin effect, and the aquifer anisotropy.

## 2. Conceptual and mathematical model

The general geometry of the problem is shown in Fig. 1. The origin of the coordinate system is at the lower boundary below the center of the horizontal wellbore, and the positive  $z$ -direction is upward. The aquifer is assumed laterally infinite but vertically finite with a thickness of  $d$ . The aquifer is homogeneous, and the principal directions of the hydraulic conductivity tensor are generally assumed to coincide with the coordinate axes. A no-flow boundary exists at the bottom, and a leaky confining layer is at the top of the aquifer. The aquifer and the fluid are slightly compressible and have constant physical properties. We assume that the horizontal well has a finite-diameter and a finite screen length. The central axis of the well is along the  $x$ -axis from  $-L/2$  to  $L/2$ , where  $L$  is the screen length of the horizontal wellbore, and the cross-section of the horizontal well is a circular area with the diameter of  $2r_w$ . The depth from the central axis of the horizontal well to the lower boundary is  $z_w$ .

We separate the problem-solving process into two parts (the rationale of doing so is explained later in

Section 2.1). The first part is finding the geometric function (GF) that is related to the geometry of the well and characteristics of the aquifer. In this part, we study ground water flow to a point source first, and then superpose the point source solution to obtain the solution of a horizontal well. The second part of the process is about the source function (SF) that includes the production rate, wellbore storage, and skin effect.

Now we briefly discuss the way to handle the leaky aquifer. Hantush [16, p. 348] pointed out that studying flow in a leaky aquifer must consider a combined problem of flow in the leaky aquifer, flow in the leaky confining layer, and flow in the adjacent aquifer simultaneously. The solution of this problem is difficult to use in practice. Hantush [16] suggested that the leakage may be substituted as a source/sink which is located inside the aquifer whose boundary is fully impermeable. We should point out that Hantush's assumption [16, p. 348] about leakage is usually thought to be "sufficiently accurate for practical purposes" for the vertical well solutions developed by him. However, whether this assumption is accurate enough for a horizontal-well problem is unknown. If treating a finite-length, finite-diameter horizontal well as a superposition of many partially penetrating vertical wells whose screen lengths equal the diameter of the horizontal well, then it is reasonable to extend Hantush's assumption to a horizontal-well problem. In this study, we assume that such a treatment is sufficiently accurate for practical purposes for a horizontal as well as vertical wellbore.

The hydrological system is assumed to be static before pumping; thus the initial hydraulic head of the leaky aquifer equals the head in the adjacent aquifer above the leaky confining layer ( $h_0$ ). Based on this, the governing equation of ground water flow to a point source in a three-dimensionally anisotropic leaky aquifer is [16]

$$K_x \frac{\partial^2 h}{\partial x^2} + K_y \frac{\partial^2 h}{\partial y^2} + K_z \frac{\partial^2 h}{\partial z^2} - K' \frac{h_0 - h}{d'} - S_s \frac{\partial h}{\partial t} = q_f(t) \delta(x - x_0) \delta(y - y_0) \delta(z - z_0), \quad (1)$$

where  $K_x, K_y, K_z$  are the principal hydraulic conductivities (m/s) in the  $x$ -,  $y$ -, and  $z$ -directions, respectively,  $h$  is the hydraulic head (m),  $K'$  is the hydraulic conductivity of the leaky confining layer (m/s),  $h_0$  is the head in the adjacent aquifer above the leaky confining layer and is assumed to be constant (m),  $d$  and  $d'$  are the thickness of the leaky aquifer and the leaky confining layer, respectively,  $S_s$  is the specific storativity of the aquifer ( $m^{-1}$ ),  $t$  is the time (s),  $q_f$  is the aquifer pumping rate for a point source ( $m^3/s$ ) ( $q_f > 0$  means pumping),  $\delta(u)$  is the Dirac delta function, and  $(x_0, y_0, z_0)$  is the point source location.

The outer boundaries that are located at infinity from the source along the horizontal directions are

$$h(x, y, z, t)|_{x=\pm\infty} = h_0, \quad h(x, y, z, t)|_{y=\pm\infty} = h_0, \quad (2)$$

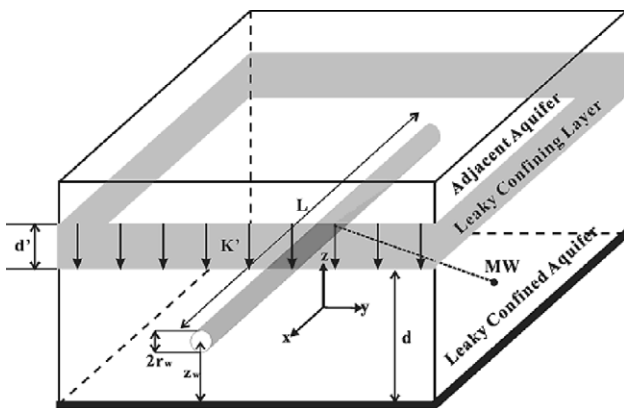


Fig. 1. General geometry of a finite-diameter horizontal well in a homogeneous, anisotropic, leaky confined aquifer. A leaky confining layer separates the leaky confined aquifer from an adjacent aquifer. MW is the location of the monitoring point.

and the conditions at the upper and lower boundaries are

$$\partial h(x, y, z, t) / \partial z|_{z=0} = 0, \quad \partial h(x, y, z, t) / \partial z|_{z=d} = 0. \quad (3)$$

The initial condition is

$$h(x, y, z, t)|_{t=0} = h_0. \quad (4)$$

If  $K'/d' \rightarrow 0$ , Eq. (1) converges into the governing equation of a confined aquifer.

### 2.1. Solution in a leaky aquifer

For the convenience of calculation, we change the variable from head,  $h$ , to drawdown,  $s = h_0 - h$ , and define the dimensionless parameters in Table 1 where all the parameters are explained in the nomenclature. The solution of Eq. (1) can be obtained either using a Laplace transform [9,28,29] or Green's function method [13,35]. By applying a Laplace transform to Eqs. (1)–(4) and using the above-defined dimensionless parameters, one has

$$p\bar{s}'_D = \frac{\partial^2 \bar{s}'_D}{\partial x_D^2} + \frac{\partial^2 \bar{s}'_D}{\partial y_D^2} + \frac{\partial^2 \bar{s}'_D}{\partial z_D^2} + 4\pi\bar{q}'_{fD}(p) \times \delta(x_D - x_{0D})\delta(y_D - y_{0D})\delta(z_D - z_{0D}), \quad (5)$$

$$\partial \bar{s}'_D(x_D, y_D, 0, p) / \partial z_D = 0, \quad (6)$$

$$\partial \bar{s}'_D(x_D, y_D, 1, p) / \partial z_D = 0, \quad (7)$$

Table 1  
Dimensionless terms defined for this study

---

$B_D^2 = \frac{K_z d'}{K' r_d},$
$L_D = \frac{L}{d} \sqrt{\frac{K_z}{K_x}},$
$q_{fD} = \frac{q_f}{q},$
$q'_{fD} = q_{fD} \exp\left(\frac{t_D}{B_D^2}\right),$
$Q_{fD} = Q_f / Q,$
$Q_{wD} = Q_w / Q,$
$r_{wD} = r_w / d,$
$s_D = \frac{4\pi\sqrt{K_x K_y} d}{q} s,$
$s'_D = s_D \exp\left(\frac{t_D}{B_D^2}\right),$
$t_D = \frac{K_z}{S_x d^2} t,$
$x_D = \frac{x}{d} \sqrt{\frac{K_z}{K_x}}, \quad y_D = \frac{y}{d} \sqrt{\frac{K_z}{K_y}}, \quad z_D = \frac{z}{d},$
$\alpha = \frac{r_w L C_s}{2d\sqrt{K_x K_y}},$
$\beta = \frac{4\sqrt{K_x K_y} S_x d^3}{K_z r_c^2}.$

---

$$\bar{s}'_D(\pm\infty, y_D, z_D, p) = \bar{s}'_D(x_D, \pm\infty, z_D, p) = 0, \quad (8)$$

where  $p$  is the Laplace transform variable referred to as the dimensionless time, over bar means Laplace transformation,  $s'_D$  and  $q'_{fD}$  are defined in Table 1, and  $x_{0D}$ ,  $y_{0D}$ , and  $z_{0D}$  are defined in the same way as  $x_D$ ,  $y_D$ , and  $z_D$ , respectively.

Eqs. (5)–(8) are solved in Appendix A, and the dimensionless drawdown is

$$s_D(t_D) = \int_0^{t_D} q_{fD}(t_D - \tau) \exp\left[-\frac{\tau}{B_D^2} - \frac{r_D^2}{4\tau}\right] \times \left[1 + 2 \sum_{n=1}^{\infty} \cos[n\pi z_D] \cos[n\pi z_{0D}]\right] \times \exp[-n^2 \pi^2 \tau] \frac{d\tau}{\tau}, \quad (9)$$

where  $r_D$  is the dimensionless horizontal distance from point source to monitoring location, and  $B_D^2$  is defined in Table 1.

The first term inside the integration sign of Eq. (9),  $q_{fD}(t_D - \tau)$  is the source function (SF) for a point source; while the product of all the rest of the terms inside the integration sign of Eq. (9) is the dimensionless point geometric function,  $g_0(x_D, y_D, z_D; x_{0D}, y_{0D}, z_{0D}, t_D)$ :

$$g_0(x_D, y_D, z_D; x_{0D}, y_{0D}, z_{0D}, t_D) = \exp\left[-\frac{t_D}{B_D^2} - \frac{r_D^2}{4t_D}\right] \left[1 + 2 \sum_{n=1}^{\infty} \cos[n\pi z_D] \cos[n\pi z_{0D}]\right] \times \exp[-n^2 \pi^2 t_D] \frac{1}{t_D}, \quad (10)$$

and in Laplace domain

$$\bar{g}_0(x_D, y_D, z_D; x_{0D}, y_{0D}, z_{0D}, p) = 2K_0 \left(r_D \sqrt{p + 1/B_D^2}\right) + 4 \sum_{n=1}^{\infty} \cos[n\pi z_D] \times \cos[n\pi z_{0D}] K_0 \left(r_D \sqrt{p + n^2 \pi^2 + 1/B_D^2}\right), \quad (11)$$

where  $\bar{g}_0$  is the Laplace transform of  $g_0$ ,  $K_0$  is the second kind, zero-order modified Bessel function. Eq. (9) indicates that the dimensionless drawdown is simply the convolution of the source function and geometric function in dimensionless time domain. If represented in Laplace domain, the dimensionless drawdown is the product of source function and geometric function. Such a problem-solving mechanism can be extended to other types of sources such as line or volume sources. One can reproduce the line source solution of a partially penetrating vertical well in a leaky aquifer [2, p. 349,16, p. 350] by integrating  $z_{0D}$  along the vertical direction of Eq. (9).

2.2. Solution for a point source in a confined aquifer

As a special case of the leaky aquifer solution, if assuming that the conductance of the leaky confining layer,  $K'/d'$ , goes to zero, Eq. (1) becomes the governing equation of flow in a confined aquifer and Eq. (9) reduces to the solution for a confined aquifer. By assigning  $B_D \rightarrow \infty$  in Eq. (9), one obtains

$$s_D(x_D, y_D, z_D; x_{0D}, y_{0D}, z_{0D}, t_D) = \int_0^{t_D} q_{fD}(t_D - \tau) \exp\left[\frac{-r_D^2}{4\tau}\right] \times \left[1 + 2 \sum_{n=1}^{\infty} \cos[n\pi z_D] \cos[n\pi z_{0D}] \exp[-n^2\pi^2\tau]\right] \frac{d\tau}{\tau}, \tag{12}$$

which is the point source solution in a confined aquifer.

3. Solution of a finite-diameter horizontal well with wellbore storage and skin effect

The point source solution (Eq. (9)) is the foundation for the following work. A finite-diameter horizontal well can be visualized as superposition of many point sources, and the aquifer pumping rate from the horizontal well,  $Q_f$ , is defined as

$$Q_f(t) = \frac{1}{V} \int_V q_f(x, y, z, t) dV, \tag{13}$$

where  $V$  is the volume of the horizontal wellbore and  $q_f(x, y, z, t)/V$  is the point source strength. Before proceeding, we need to answer the following two questions:

1. How is the pumping rate distributed inside a horizontal wellbore?
2. How is the aquifer pumping rate,  $Q_f(t)$ , related to the total pumping rate,  $Q$ , and the pumping time?

3.1. Pumping rate distribution inside a horizontal well

There are traditionally two different methods to treat a pumping well. One method is to treat it as a uniform flux boundary, and another is to treat it as a uniform head boundary. Hantush [16] pointed out that these two treatments were two extremes and a realistic wellbore was a mixed-type boundary between these two extremes because of flow inside the wellbore. Several researches have studied the mixed-type boundary value problems for the partially penetrating vertical well [6,14,23,32]. In recent years, great advancements have been made in using the mixed-type boundary to treat a vertical wellbore [3,4,41,49]. Intensive computational power is still needed to perform the numerical calculation when using this method. No effort is made in this study to incorporate the mixed-type boundary method to treat the

horizontal wellbore. However, because the mixed-type boundary is assumed to be closer to the physical boundary, additional research is needed to apply this method for horizontal-well study in the future.

As a result, scientists favor the uniform flux boundary because of its simple implementation in the analytical study. However, the true distribution of pumping rate is non-uniform because the pumping rate at both ends of the screen is higher than the average over the screen length. Thus, it is important to know the errors associated with the uniform flux boundary assumption. Previous studies indicated that the error is usually less than a few percent if the screen length-to-well radius is large enough:  $L/r_w > 40$  [6,41]. This condition is almost always satisfied for a horizontal pumping well case because the horizontal wells used in hydrological and environmental studies usually have long screen lengths. Because of this, the uniform flux boundary can be safely used for treating horizontal wells in practical cases. If using the uniform flux to treat a horizontal well,  $q_f(x, y, z, t)$  in Eq. (13) is independent of  $(x, y, z)$ , and Eq. (13) becomes  $Q_f(t) = q_f(t)$ .

3.2. Consideration of wellbore storage and skin effect

The wellbore storage is one of the important parameters that mask early time or near to pumping well pressure data by distorting the aquifer water levels in pumping tests [28,40,48].

The total pumping rate,  $Q$ , is the summation of the aquifer pumping rate,  $Q_f(t)$ , and the wellbore storage pumping rate,  $Q_w(t)$ :  $Q_w(t) + Q_f(t) = Q$ . The wellbore storage supplies most of the initial pumped water, and  $Q_w(t)$  initially equals  $Q$  and gradually decreases to zero when pumping continues [47]

$$Q_w = \pi r_c^2 \frac{\partial s_w}{\partial t}, \tag{14}$$

where  $r_c$  is the radius of the casing connected with the horizontal-well screen, and  $s_w$  is the drawdown inside the wellbore.  $r_c$  may or may not be equal to the radius of the horizontal-well screen,  $r_w$ . In contrast,  $Q_f(t)$  is initially zero and gradually approaches  $Q$  when pumping continues. Using Darcy's Law, the aquifer-pumping rate is proportional to the head difference at wellbore [9,28,47]:

$$Q_f = (2\pi r_w L C_s)(s_w - f), \tag{15}$$

where  $L$  is the screen length of the horizontal well,  $C_s$  is the conductance of wellbore skin ( $K_s/d_s$ ),  $K_s$  and  $d_s$  are the hydraulic conductivity and the thickness of the skin, respectively, and  $f$  is the averaged drawdown at the outside surface of the wellbore skin.

The skin is assumed to be infinitesimally thin when using Eq. (15). This treatment is similar to those used by Dougherty and Babu [9], Ehlig-Economides and Joseph [10], Kabala and Cassiani [22], and many others in

studying vertical wells. However, it is different from the finite-thickness skin effect treatment used by Novakowski [34], and Moench and Hsieh [30]. Using the similar notation employed by Kabala and Cassiani [22] to define the skin effect,  $\eta$ , in an isotropic aquifer:

$$-\eta r_w \frac{\partial f(r_w, t)}{\partial r} + f(r_w, t) = s_w, \tag{16}$$

and recall Darcy’s Law:  $Q_f = -2\pi r_w LK(\partial f/\partial r)$ , where  $K$  is the aquifer hydraulic conductivity, then the skin effect corresponding to Eq. (15) becomes

$$\eta = \frac{K}{r_w C_s}. \tag{17}$$

Using the notation of Moench and Hsieh [30], defining  $r_s = r_w + d_s$ , and considering an infinitesimal skin, then  $\lim_{d \rightarrow 0} \ln[r_s/r_w] = \lim_{d \rightarrow 0} \ln[(r_w + d_s)/r_w] \simeq d_s/r_w$ . Thus the skin effect given by Moench and Hsieh [30] becomes

$$\eta = \frac{K}{K_s} \ln[r_s/r_w] \simeq \frac{K}{K_s} \times \frac{d_s}{r_w} = \frac{K}{r_w C_s},$$

which is identical to our Eq. (17).

The dimensionless form of Eq. (15) becomes

$$Q_{fD} = \alpha [s_{wD} - f_D(t)], \tag{18}$$

where  $Q_{fD}$  and  $\alpha$  are defined in Table 1, and  $s_{wD}$  and  $f_D$  are defined in the same way as the dimensionless drawdown given in Table 1. The dimensionless wellbore pumping rate is

$$Q_{wD} = \partial s_{wD} / \beta \partial t_D, \tag{19}$$

where  $Q_{wD}$  and  $\beta$  are defined in Table 1.

The summation of  $Q_{fD}$  and  $Q_{wD}$  is

$$Q_{wD} + Q_{fD} = 1. \tag{20}$$

Substituting Eqs. (18) and (19) into Eq. (20) results in a differential equation of  $s_{wD}$ . Solving the equation in Laplace domain and substituting the solution of  $s_{wD}$  into Eq. (18) results in

$$\bar{Q}_{fD}(p) = -\frac{\alpha p \bar{f}_D(p)}{p + \alpha \beta} + \frac{1}{p} - \frac{1}{p + \alpha \beta}, \tag{21}$$

where the over bar implies the Laplace transform. The average drawdown (in Laplace domain) at the wellbore screen face is  $\bar{f}_D(p) = \bar{Q}_{fD}(p) \bar{g}^*(p)$ , where  $\bar{g}^*(p)$  is the surface average of the geometric function of the finite-diameter well along the wellbore screen face in Laplace domain. The geometric function of the finite-diameter well in Laplace domain,  $\bar{g}(x_D, y_D, z_D, p)$ , is

$$\bar{g}(x_D, y_D, z_D, p) = \frac{1}{V} \int_V \bar{g}_0(x_D, y_D, z_D; x_{0D}, y_{0D}, z_{0D}, p) dV, \tag{22}$$

where  $\bar{g}_0(x_D, y_D, z_D; x_{0D}, y_{0D}, z_{0D}, p)$  is the point geometric function in Laplace domain defined in Eq. (11).

Therefore Eq. (21) becomes

$$\bar{Q}_{fD}(p) = -\frac{\alpha p \bar{Q}_{fD}(p) \bar{g}^*(p)}{p + \alpha \beta} + \frac{1}{p} - \frac{1}{p + \alpha \beta}. \tag{23}$$

The resultant solution of the source function in Laplace domain is

$$\bar{Q}_{fD}(p) = \frac{\alpha \beta}{p[p\{1 + \alpha \bar{g}^*(p)\} + \alpha \beta]}. \tag{24}$$

Two special cases deserve discussion:

1. If the well has a negligible wellbore storage, i.e.,  $r_c \rightarrow 0$  and  $\beta \rightarrow \infty$ , Eq. (24) converges to  $\bar{Q}_{fD}(p) = 1/p$ , which yields the constant pumping rate.
2. If the skin effect is negligible but the wellbore storage is not, i.e.,  $d_s \rightarrow 0$ , so  $\alpha \rightarrow \infty$ , Eq. (24) becomes  $\bar{Q}_{fD}(p) \rightarrow \beta/[p\{p\bar{g}^*(p) + \beta\}]$ , which yields the pumping rate without skin.

### 3.3. Solution of a finite-diameter horizontal well

Eq. (24) indicates that if  $\bar{g}^*(p)$  is known, then the aquifer pumping rate is also known. However, a rigorous analytical deviation of  $\bar{g}^*(p)$  is extremely difficult for a finite-diameter horizontal well because of the change of head along the outside skin of the screened section of a wellbore. Fortunately, based on the following arguments, a close approximation of  $\bar{g}^*(p)$  can be derived:

1. A finite-diameter horizontal well is a volume source that can be visualized as the superposition of many horizontal line sources. Thus the average geometric function of a finite-diameter horizontal well can be calculated from the average geometric functions of the superposed horizontal line sources.
2. Previous investigations about the horizontal line sources indicated that the drawdown at  $x_D/(L_D/2) = 0.68$  offers an excellent approximation of the average drawdown at the horizontal wellbore [7,42,52], where  $L_D$  is the dimensionless well screen length defined in Table 1. Thus the average geometric function of a line source can be calculated by substituting  $x_D/(L_D/2) = 0.68$ ,  $y_D = 0$ ,  $z_D = z_{wD}$ , and  $B_D \rightarrow \infty$  into the line source drawdown solution [52, Eq. (18)]. Considering the slight difference in the definitions of dimensionless drawdown used in [52] and in this work, the result is

$$\bar{g}^*(p) = \frac{2}{L_D} \left[ \int_{-L_D/2}^{L_D/2} K_0[\sqrt{p}|0.34L_D - x'_D|] dx'_D + 2 \sum_{n=1}^{\infty} \cos^2[n\pi z_{wD}] \int_{-L_D/2}^{L_D/2} K_0[\sqrt{p + n^2\pi^2} |0.34L_D - x'_D|] dx'_D \right]. \tag{25}$$

Eq. (25) can be simplified if considering the fact that the wellbore storage and skin effect influence the early time drawdown the most; thus the above calculation will be targeted for  $p \gg 1$ . Under that condition, using the following identity  $\int_0^u K_0(u) du \simeq \pi/2$ , if  $u \geq \pi$  [16,52], an

approximate form of the average geometric function becomes

$$\bar{g}^*(p) = \frac{2\pi}{L_D} \left\{ \frac{1}{\sqrt{p}} + 2 \sum_{n=1}^{\infty} \cos^2(n\pi z_{wD}) \frac{1}{\sqrt{p + n^2\pi^2}} \right\}. \tag{26}$$

Eq. (26) will be used as the approximate geometric function of a finite-diameter well, and it will be substituted into Eq. (24) to obtain  $\bar{Q}_{fD}(p)$ . The aquifer pumping rate  $Q_{fD}(t_D)$  is numerically obtained through the inverse Laplace transform of  $\bar{Q}_{fD}(p)$  using the Stehfest algorithm [46].

With these preparations, one can now calculate the drawdown near a finite-diameter horizontal pumping well by the volume integration of the point source solution:

$$s_{HD}(t_D) = \frac{1}{V} \int s_D(t_D) dx_0 dy_0 dz_0 = \frac{d^3 \sqrt{K_x K_y} / K_z}{\pi r_w^2 L} \int s_D(t_D) dx_{0D} dy_{0D} dz_{0D}, \tag{27}$$

where  $s_{HD}$  is the horizontal-well dimensionless drawdown defined in Table 1 with  $q$  replaced by  $Q$ . After performing the spatial integration, Eq. (27) becomes

$$s_{HD}(t_D) = \frac{\sqrt{K_y/K_z}}{L_D r_{wD}^2} \int_0^{t_D} Q_{fD}(t_D - \tau) \exp\left(-\frac{\tau}{B_D^2}\right) \times \{\text{erf}(\lambda_1) + \text{erf}(\lambda_2)\} \times \int_{z_{wD} - r_{wD}}^{z_{wD} + r_{wD}} \{\text{erf}(\mu_1) + \text{erf}(\mu_2)\} \times \left\{ 1 + 2 \sum_{n=1}^{\infty} \cos(n\pi z_D) \cos(n\pi z_{0D}) \times \exp(-n^2\pi^2\tau) \right\} dz_{0D} d\tau, \tag{28}$$

where  $r_{wD}$  is defined in Table 1; the aquifer pumping rate,  $Q_{fD}(t_D)$ , is the inverse Laplace transform of Eq. (24); and

$$\lambda_1 = \frac{L_D/2 + x_D}{2\sqrt{\tau}}, \quad \lambda_2 = \frac{L_D/2 - x_D}{2\sqrt{\tau}},$$

$$\mu_1 = \frac{\sqrt{r_{wD}^2 - (z_{0D} - z_{wD})^2} \sqrt{K_z/K_y} + y_D}{2\sqrt{\tau}},$$

$$\mu_2 = \frac{\sqrt{r_{wD}^2 - (z_{0D} - z_{wD})^2} \sqrt{K_z/K_y} - y_D}{2\sqrt{\tau}}.$$

When the well radius  $r_{wD} \rightarrow 0$ , Eq. (28) is simplified to

$$s_{HD}(t_D) = \frac{\sqrt{\pi}}{L_D} \int_0^{t_D} Q_{fD}(t_D - \tau) \exp\left(-\frac{\tau}{B_D^2}\right) \times \{\text{erf}(\lambda_1) + \text{erf}(\lambda_2)\} \times \exp\left(-\frac{y_D^2}{4\tau}\right) \times \left[ 1 + 2 \sum_{n=1}^{\infty} \cos(n\pi z_D) \cos(n\pi z_{wD}) \times \exp(-n^2\pi^2\tau) \right] \frac{d\tau}{\sqrt{\tau}}. \tag{29}$$

Eq. (29) is the line source solution including the wellbore storage, skin effect, and leakage. If excluding the wellbore storage, skin effect, and leakage, then Eq. (29) is identical to the solution derived by Zhan et al. [52] if taking into account the slightly different definitions of the dimensionless drawdowns (we used  $s_D = 4\pi d \sqrt{K_x K_y} s / q$ , and Zhan et al. [52] used  $s_D = 2\pi d \sqrt{K_x K_y} s / q$ ).

For a confined aquifer,  $B_D^2$  goes to infinity, the second term in Eq. (28) converges to unity, and the drawdown near a horizontal well in a confined aquifer is obtained.

#### 4. Results and discussion

The integration in Eq. (28) is computed using a numerical integration scheme [37]. The numerical evaluation of the drawdown is accomplished using a MATLAB® program developed by the authors. This program, named FINHOW, together with the user's manual, is available from the authors' website: <http://park.tamu.edu/research.htm> and <http://geoweb.tamu.edu/Faculty/Zhan/Research.html> or by individual contact. This program is devised to calculate and plot a time-dependent drawdown curve at any measuring point in a leaky or confined aquifer near a horizontal well.

The influence of the finite well radius on the flow is most significant at near fields defined as the regions close to the horizontal well. The influence of the wellbore storage is most important at the early time during which the water is withdrawn from near fields. Thus in the following discussion, we will focus on the drawdown change at the near field and/or at the early time.

Many interesting aspects of the results are shown in Figs. 2–7. If not specified, the following default values of parameters are used in those figures: aquifer thickness is 10 m; aquifer is homogeneous and isotropic with hydraulic conductivities equal to 0.0001 m/s; specific storativity is 0.0002 m<sup>-1</sup>; horizontal well is 100 m long and located at the middle elevation of the aquifer ( $z_w = 5$  m); pumping rate is 0.01 m<sup>3</sup>/s; well radius is 0.1 m; for simplicity, the casing radius,  $r_c$ , is assumed to be the same as the horizontal-well radius,  $r_w$ , in the following discussion; conductance of the wellbore skin is 0.001 s<sup>-1</sup> if skin effect is included; and monitoring point is at the same elevation as the horizontal well and is very close to the well at (1 m, 1 m, 5 m). For brevity of illustration, confined condition is used in most cases except that in Section 4.5.

Fig. 2 is the plot of dimensionless drawdown versus dimensionless time in a semi-log paper, and it shows three distinct sections reflecting the early flow, where all the direction of the flow caused by the pumping is perpendicular to the surface of the screened section, the intermediate transitional flow, where the drawdown is affected by the upper and lower boundaries, and the later time pseudo-radial flow. This result is identical to

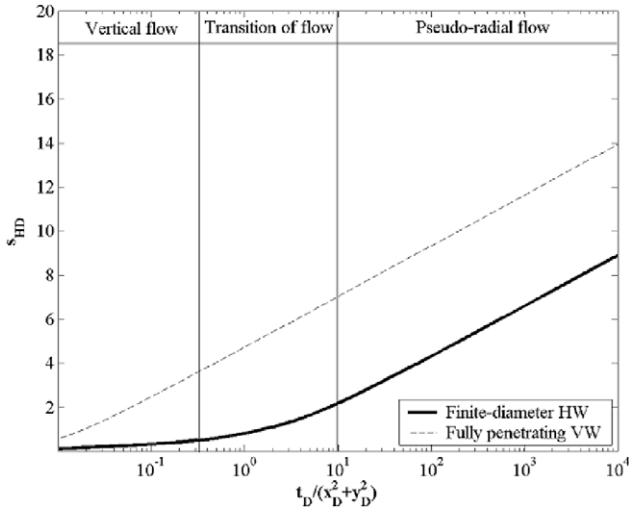


Fig. 2. Comparison of dimensionless semi-log type curves of a finite-diameter horizontal well (HW) and a fully penetrating vertical well (VW).

those found in previous studies using a line source, and the mechanism of this changing flow from vertical radial to pseudo-radial is explained thoroughly in previous works [7,12,24,52]. Leakage effect is excluded in the following figures except Fig. 7.

4.1. Effect of well radius on geometric function

The simulation of changing in the value of dimensionless geometric function with dimensionless time of different well radii in an isotropic aquifer is performed, and the results are shown in Fig. 3. We tested the dimensionless well radii of 0.01, 0.04, 0.07, and 0.1. Wellbore storage and skin effects are excluded in this section. The purpose here is to compare our volume

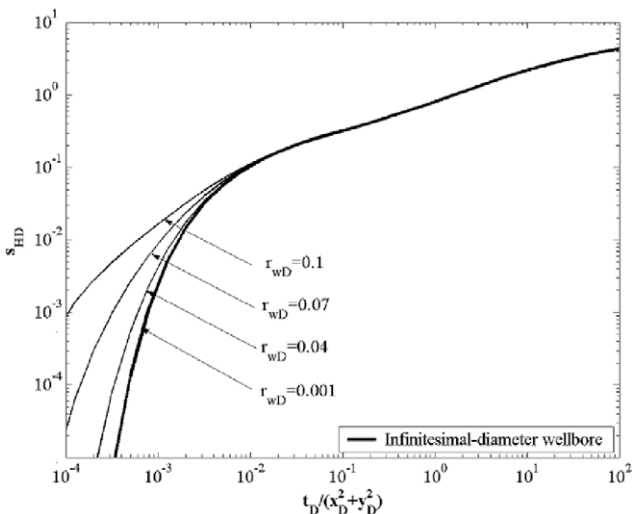


Fig. 3. Dimensionless type curves with different wellbore radii in an isotropic aquifer. Wellbore storage and skin effects are excluded.

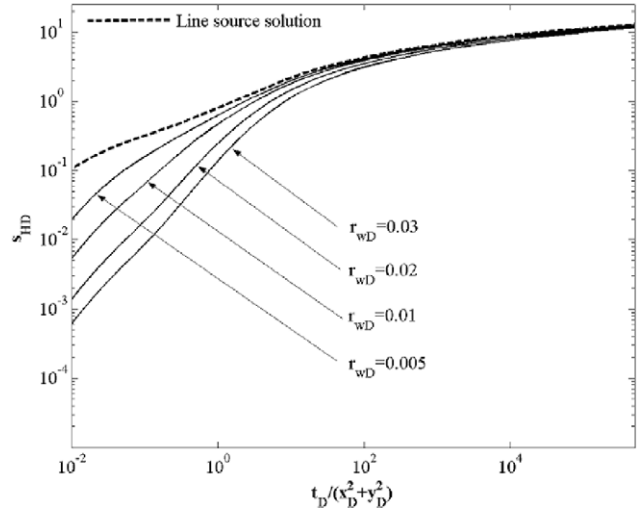


Fig. 4. Comparison of dimensionless type curves with different dimensionless wellbore radii and the dimensionless type curve of the line source solution derived by Zhan et al. [52] in an isotropic aquifer. Wellbore storage and skin effects are included.

source solution Eq. (28) to a previous line source solution developed by Zhan et al. [52].

The influence of the finite-diameter of the well on the geometric function in the near field case should be most profound at the early time during which water is withdrawn from the near field storage. When pumping time increases, the contribution to the geometric function comes from water withdrawn from fields with progressively increasing distances to the well, and the geometric function of the finite-diameter of the well will play a less important role. This rationale is verified in Fig. 3, which shows that the finite-diameter well solution converges to the line source solution very fast in the isotropic case. After  $t_D/(x_D^2 + y_D^2) = 0.01$ , the line source solution can

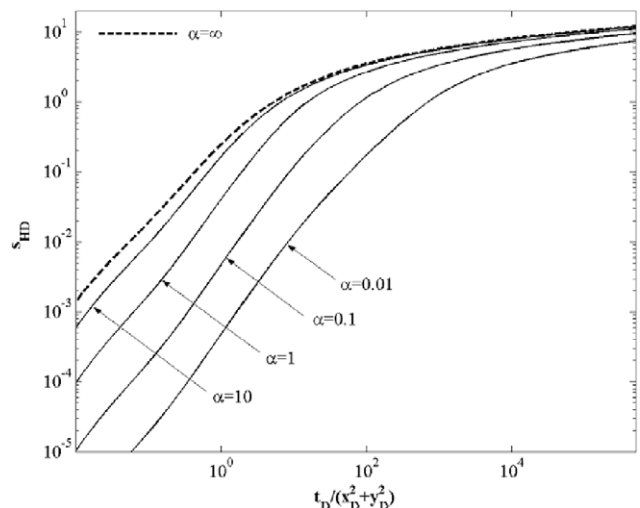


Fig. 5. Dimensionless type curves with different skin effects.  $\alpha \rightarrow \infty$  refers to the no-skin case.

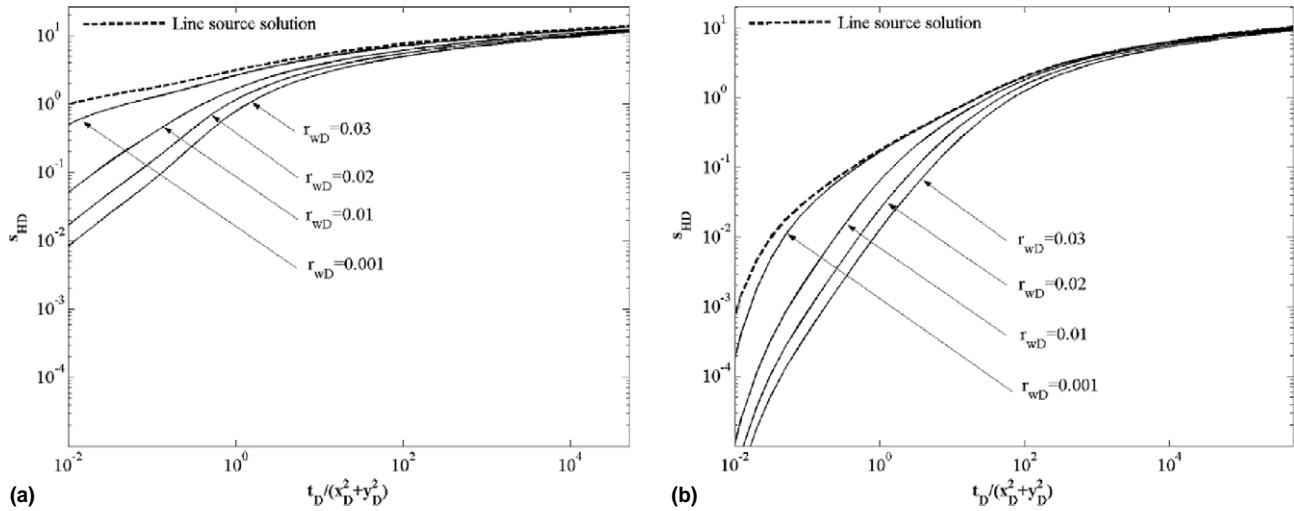


Fig. 6. Comparison of dimensionless type curves with different wellbore radii and the dimensionless type curve of the line source solution derived by Zhan et al. [52] in an anisotropic aquifer. (A)  $K_z/K_x = 0.1$ ; (B)  $K_z/K_x = 10$ , and  $K_x = K_y$  for both (A) and (B). Wellbore storage and skin effects are included.

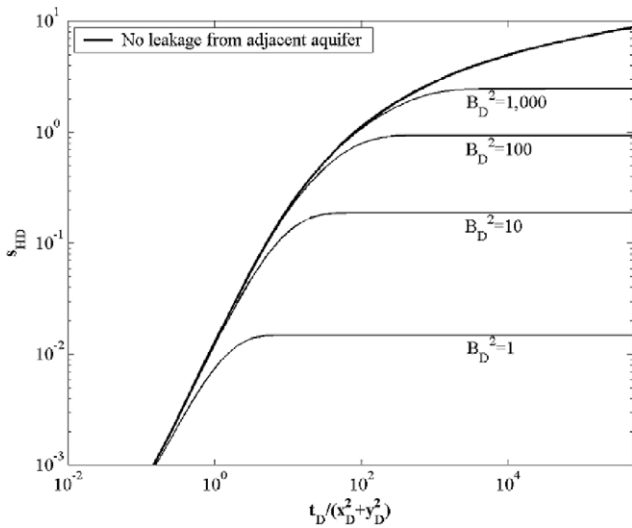


Fig. 7. Comparison of dimensionless type curves with different leakage parameters and the dimensionless type curve of the line source solution derived by Zhan et al. [52] in an isotropic aquifer. Wellbore storage and skin effects are included.

be safely used for a finite-diameter well case in an isotropic aquifer. Substituting the assigned parameters into  $t_D/(x_D^2/y_D^2) = 0.01$  results in  $t = 0.04$  s. Thus, we prove that for any practical purpose, the volume-source geometric function can be safely replaced by the line-source geometric function, and Eq. (29) can be used to replace Eq. (28) for practical calculations.

4.2. Effect of wellbore storage

Given the same skin conductance of  $10^{-4}/s$ , a different well radius means a different wellbore storage. If the

effect of wellbore storage is included, water withdrawn in the initial pumping is mostly from the wellbore storage and less from the aquifer storage; thus the drawdown at the monitoring well should be much smaller than that in Fig. 3 at the early time. With increasing pumping time, the wellbore storage is gradually depleted and more water is withdrawn from the near field, and we should observe a rapid increase of drawdown. Thus, compared to the case excluding the wellbore storage (such as Fig. 3), it seems that the influence of the horizontal well diameter on the drawdown is delayed by a period of time during which the wellbore storage supplies more water to the pumping than the aquifer. The largest well diameter has the longest delay. The masked section of the drawdown curve has almost a straight line with a unit slope when most of the water is deduced from wellbore. This coincides with previous works [36,47]. This explanation is reflected in Fig. 4. This finding is similar to those observed in vertical-well problems [47, p. 52, Fig. 2.2].

4.3. Effect of skin

The wellbore storage effect deforms the early drawdown, and it depends on two parameters: the volume of the pumping wellbore and the conductance of the well skin  $K_s/d_s$ . Given the same wellbore volume, a higher skin conductance implies easier flow of water from the aquifer to the well and the rapid transformation of water withdrawal from the wellbore to the water withdrawal from the aquifer.

The sensitivity analysis of drawdown to the skin effect is tested with different skin conductance  $K_s/d_s$ . The aforementioned effect of masking early time drawdown by the skin effect is observed in Fig. 5. By the analysis,

one can find that the lower conductance of the skin causes less drawdown and longer delay of response to the pumping in the aquifer at early time. That is because it is difficult for groundwater to penetrate a lower conductance skin. When the skin conductance increases, the drawdown becomes less and less sensitive to the conductance and the type curves approach the asymptotic limit with an infinite conductance. In fact, Fig. 5 shows that when the conductance is larger than  $10^{-4}/s$ , the skin effect can be negligible for the given monitoring point.

#### 4.4. Effect of anisotropy

The anisotropic aquifer used in Fig. 6(a) has horizontal hydraulic conductivity of 0.0001 m/s and vertical hydraulic conductivity 0.00001 m/s; while the horizontal hydraulic conductivity, 0.00001 m/s, and vertical hydraulic conductivity, 0.0001 m/s, are used in Fig. 6(b). Both wellbore storage and skin effects are included in this section. The ratio of vertical versus horizontal hydraulic conductivity is commonly found in the range of 0.01–1 in many rock types [8, p. 40]. If vertical fractures dominate, the vertical hydraulic conductivity could be larger than the horizontal hydraulic conductivity, and the ratio of vertical versus horizontal hydraulic conductivity could vary over a few orders of magnitude in such a fractured aquifer. Similarly, if horizontal fractures dominate in a certain orientation, the ratio of  $K_x/K_y$  could also vary over a few orders of magnitude in such a fractured aquifer.

If vertical hydraulic conductivity is much less than the horizontal hydraulic conductivity, it is more difficult to drain the water vertically; thus most water flow to the well comes from the horizontal direction, and we should observe larger drawdowns at the horizontal near field at the early time if compared to the isotropic case. This is true by comparing Fig. 6(a) to Fig. 4. On the contrary, if vertical hydraulic conductivity is larger than the horizontal hydraulic conductivity, it is easier to drain the water vertically; thus we should observe smaller drawdowns at the horizontal near field at the early time if compared to the isotropic case. This is confirmed by comparing Fig. 6(b) to Fig. 4. Figs. 6(a) and (b) indicate that the near field drawdown curves at the early time strongly depend on the vertical anisotropy because of the strong vertical flow near a horizontal well.

#### 4.5. Effect of leaky aquifer

The sensitivity analysis of drawdown to leaking parameters is tested using five different leakage parameters  $B_D^2$ , and the results are shown in Fig. 7. The wellbore storage and skin effects are included in this section. The drawdowns in leaky aquifers follow similar curves ob-

served in vertical well problems [47] at the late time when the water across the leaking bed becomes significant. The early and the intermediate time stages follow the same curves as that in the confined aquifers. In the case of the storage of the aquitard being considered, more complicated drawdown mechanisms are expected on the early and intermediate time stages. Further investigations including the aquitard storage are needed to provide better solutions to the problems in which the aquitard storage cannot be neglected. If the leakage parameter,  $B_D^2$ , goes to infinity, the leaky aquifer solution approaches that of the confined aquifer.

## 5. Summary and conclusions

This paper provides solutions on groundwater flow to a finite-diameter horizontal well including wellbore storage and skin effect. These solutions offer better physical insights than previous line source solutions into the hydraulics of horizontal wells in three-dimensionally anisotropic leaky aquifers. They are more useful for describing the near field drawdown behavior.

The drawdown solution for a finite-diameter horizontal well is derived on the basis of volume integration of point-source solutions. A graphically integrated numerical MATLAB<sup>®</sup> program named FINHOW is written by the authors to compute the volume integration using the Gaussian quadrature method [37] and to provide the type curves of groundwater flow to a finite-diameter horizontal well. The drawdown solution in a confined aquifer is obtained as a special case of the solution in the leaky aquifer. Our solution shows that the finite-diameter of the well only influences the near field at the early flow time. The finite-diameter solution converges to the line source solution at  $t_D/(x_D^2 + y_D^2) = 0.01$  in an isotropic aquifer if excluding the wellbore storage. If the wellbore storage is included, it will take a much longer time for the finite-diameter solution to converge to the line source solution.

The skin effect impacts flow through the conductance of the wellbore skin. A higher skin conductance means easier flow from the aquifer to the well and quicker response of the aquifer to the pumping. When the skin conductance increases, the drawdown becomes less and less sensitive to the skin conductance, and the type curves approach the asymptotic limit that is corresponding to an infinite conductance case.

The anisotropy controls the relative strength of vertical and horizontal flows at the early time, and thus shows a strong influence on the early time near-field drawdown. The leakage parameter influences the late pseudo-radial flow substantially but has limited impact on the early and intermediate flows when excluding the storage in the leaky confining layer.

**Acknowledgements**

Support for this work was provided by the US National Science Foundation Grant No. BES-9909964, research grant of the Geological Society of America Grant No. 6980-01, and by the Office of the Vice President for Research and Associate Provost for Graduate Studies at Texas A&M University through the Interdisciplinary Research Initiatives. We thank Kueyoung Kim and Beverly C. Dawkins for technical support. We thank three anonymous reviewers for their detailed and very constructive comments on this manuscript.

**Appendix A. Derivation of Eq. (9)**

Eqs. (5)–(8) are solved using the procedure described in the appendix of Zhan et al. [52]. The solution satisfying boundary conditions (6) and (7) can be written (e.g. [9,28,29]):

$$\bar{s}'_D(p) = \sum_{n=0}^{\infty} H_n(x_D, y_D, p) \cos(\omega_n z_D), \tag{A.1}$$

where  $H_n$  is a function depending on the horizontal coordinates and  $p$ , and  $\omega_n$  is the spatial frequency term. The solution is [52]:

$$H_0 = 2\bar{q}'_{fD}(p)K_0(r_D\sqrt{p}), \tag{A.2}$$

$$H_n = 4\bar{q}'_{fD}(p) \cos(n\pi z_{0D})K_0(r_D\sqrt{n^2\pi^2 + p}), \quad n > 0, \tag{A.3}$$

where  $r_D = [(x_D - x_{0D})^2 + (y_D - y_{0D})^2]^{1/2}$  is the dimensionless horizontal radial distance between the source point and measuring point, and  $K_0(u)$  is the second kind, zero-order modified Bessel function. Substituting (A.2) and (A.3) into (A.1) results in the solution of  $\bar{s}'_D$ . Applying inverse Laplace transform to the solution of  $\bar{s}'_D$  and using the following identities [16, p. 303]

$$L^{-1}(K_0(r_D\sqrt{p})) = \frac{1}{2t_D} \exp\left(-\frac{r_D^2}{4t_D}\right),$$

$$L^{-1}\left(K_0\left(r_D\sqrt{p + n^2\pi^2}\right)\right) = \frac{1}{2t_D} \exp\left(-n^2\pi^2 t_D - \frac{r_D^2}{4t_D}\right), \tag{A.4}$$

and the convolution theorem, where  $L^{-1}$  is the inverse Laplace operator, one obtains

$$s'_D(t_D) = \int_0^{t_D} q'_{fD}(t_D - \tau) \exp\left[-\frac{r_D^2}{4\tau}\right] \times \left[1 + 2 \sum_{n=1}^{\infty} \cos[n\pi z_D] \cos[n\pi z_{0D}]\right] \times \exp[-n^2\pi^2\tau] \frac{d\tau}{\tau}. \tag{A.5}$$

Combining (A.5) and definitions of  $s'_D$  and  $q'_{fD}$  in Table 1, one obtains the dimensionless drawdown

$$s_D(t_D) = \int_0^{t_D} q_{fD}(t_D - \tau) \exp\left[-\frac{\tau}{B_D^2} - \frac{r_D^2}{4\tau}\right] \times \left[1 + 2 \sum_{n=1}^{\infty} \cos[n\pi z_D] \cos[n\pi z_{0D}]\right] \times \exp[-n^2\pi^2\tau] \frac{d\tau}{\tau}. \tag{A.6}$$

**References**

- [1] Agarwal RG, Al-Hussainy R, Ramey HJ. An investigation of wellbore storage and skin effect in unsteady liquid flow: I. Analytical treatment. *Soc Pet Eng J* 1970;10:279–90.
- [2] Bear J. *Hydraulics of groundwater*. New York: McGraw-Hill; 1979.
- [3] Cassiani G, Kabala ZJ. Hydraulics of a partially penetrating well: solution to a mixed-type boundary value problem via dual integral equations. *J Hydrol* 1998;211(1-4):100–11.
- [4] Cassiani G, Kabala ZJ, Medina MA. Flowing partially penetrating well: solution to a mixed-type boundary value problem. *Adv Water Resour* 1999;23(1):59–68.
- [5] Cleveland TG. Recovery performance for vertical and horizontal wells using semianalytical simulation. *Ground Water* 1994; 32(1):103–7.
- [6] Cole K, Zlotnik V. Modification of Dagan’s numerical method for slug and packer test interpretation. In: *Computational methods in water resources X*. Dordrecht, Netherlands: Kluwer Academic Publishers; 1994.
- [7] Daviau F, Mouronval G, Bourdarot G, Curutchet P. Pressure analysis for horizontal wells. *SPE Formation Eval* 1988;3(4): 716–24.
- [8] Domenico PA, Schwartz FW. *Physical and chemical hydrogeology*. second ed. New York: Wiley; 1998.
- [9] Dougherty DE, Babu DK. Flow to a partially penetrating well in a double-porosity reservoir. *Water Resour Res* 1984;20(8): 1116–22.
- [10] Ehlig-Economides C, Joseph J. A new test for determination of individual layer porosities in a multilayered reservoir. *SPE Formation Eval* 1987;261–83.
- [11] Falta RW. Analytical solutions for gas flow due to gas injection and extraction from horizontal wells. *Ground Water* 1995;33(2):235–46.
- [12] Goode PA, Thambynayagam RKM. Pressure drawdown and buildup analysis of horizontal wells in anisotropic media. *SPE Formation Eval* 1987;2(4):683–97.
- [13] Gringarten AC, Ramey HJ. The use of source and Green’s functions in solving unsteady-flow problems in reservoirs. *SPE J* 1973;13(10):285–96.
- [14] Haitjema HM, Kraemer SR. A new analytic function for modeling partially penetrating wells. *Water Resour Res* 1988; 24(5):683–90.
- [15] Hantush MS, Papadopoulos IS. Flow of ground water to collector wells. *J Hydraul Div, Proc Am Soc Civil Eng* 1962;HY 5: 221–44.
- [16] Hantush MS. *Hydraulics of wells*. In: *Advances in hydroscience*. New York: Academic Press; 1964.
- [17] Hemker CJ. Transient well flow in vertically heterogeneous aquifers. *J Hydrol* 1999;225:1–18.

- [18] Hunt B, Massmann JW. Vapor flow to trench in leaky aquifer. *J Environ Eng* 2000;126:375–80.
- [19] Jargon JR. Effect of wellbore storage and wellbore damage at the active well on interference test analysis. *J Pet Technol* 1976;28:851–8.
- [20] Jiao JJ, Rushton KR. Sensitivity of drawdown to parameters and its influence on parameter estimation for pumping tests in large-diameter wells. *Ground Water* 1995;33(5):794–800.
- [21] Joshi SD. Augmentation of well productivity with slant and horizontal wells. *J Pet Technol* 1988;729–39.
- [22] Kabala ZJ, Cassiani G. Well hydraulics with the Weber–Goldstein transforms. *Transport Porous Media* 1997;29(2):225–46.
- [23] Kirkham D. Exact theory of flow into a partially penetrating well. *J Geophys Res* 1959;64:1317–27.
- [24] Kuchuk FJ, Habashy T. Pressure behavior of horizontal wells in multilayer reservoirs with crossflow. *SPE Formation Eval* 1996;11(1):55–64.
- [25] Lai RYS, Su CW. Nonsteady flow to a large well in a leaky aquifer. *J Hydrol* 1974;22:333–45.
- [26] Maurer WC. Recent advances in horizontal drilling. *J Can Pet Technol* 1995;34(9):25–33.
- [27] Moench AF. Transient flow to a large-diameter well in an aquifer with storative semiconfining layers. *Water Resour Res* 1985;21(8):1121–31.
- [28] Moench AF. Flow to a well of finite diameter in a homogeneous, anisotropic water table aquifer. *Water Resour Res* 1997;33(6):1397–407.
- [29] Moench AF. Correction to “Flow to a well of finite diameter in a homogeneous, anisotropic water table aquifer” by A.F. Moench. *Water Resour Res* 1998;34(9):2431–2.
- [30] Moench AF, Hsieh P. Comment on “Evaluation of slug tests in wells containing a finite-thickness skin” by C.R. Faust and J.W. Mercer. *Water Resour Res* 1985;21(9):1459–61.
- [31] Murdoch LC. Transient analyses of an interceptor trench. *Water Resour Res* 1994;30(11):3023–31.
- [32] Muskat M. *The flow of homogeneous fluids through porous media*. Ann Arbor, MI: J.W. Edwards; 1937.
- [33] Ng MC, Aguilera R. Well test analysis of horizontal wells in bounded naturally fractured reservoirs. *J Can Pet Technol* 1999;38(7):20–4.
- [34] Novakowski KS. A composite analytical model of analysis of pumping tests affected by well bore storage and finite thickness skin. *Water Resour Res* 1989;25(9):1937–46.
- [35] Ozkan E, Raghavan R. New solutions for well-test-analysis problems: Part 1 – analytical consideration. *SPE Formation Eval* 1991:359–68.
- [36] Papadopoulos IS, Cooper HH. Drawdown in a well of large diameter. *Water Resour Res* 1967;3(1):241–4.
- [37] Press WH, Flannery BP, Teukolsky SA, Vetterling WT. *Numerical recipes, the art of scientific computing*. New York: Cambridge University Press; 1989.
- [38] Ramey HJ. Non-Darcy flow and wellbore storage effects in pressure buildup and drawdown of gas wells. *J Pet Technol* 1965;17:223–33.
- [39] Ramey HJ. Short-time well test data interpretation in the presence of skin effect and wellbore storage. *J Pet Technol* 1970;22:97–104.
- [40] Ramey HJ, Agarwal RG. Annulus unloading rates as influenced by wellbore storage and skin effect. *Soc Pet Eng J* 1972;12(10):453–9.
- [41] Rund NC, Kabala ZJ. Response of a partially penetrating well in a heterogeneous aquifer: integrated well-face flux vs. uniform well-face flux boundary conditions. *J Hydrol* 1997;194:76–94.
- [42] Rosa AJ, Carvalho RDS. A mathematical model for pressure evaluation in an infinite-conductivity horizontal well. *SPE Formation Eval* 1989;4(4):559–66.
- [43] Sawyer CS, Lieuallen-Dulam KK. Productivity comparison of horizontal and vertical ground water remediation well scenarios. *Ground Water* 1998;36(1):98–103.
- [44] Seines K, Lieu SC, Haug BT. Troll horizontal well tests demonstrate large production potential from thin oil zones. *SPE Reservoir Eng* 1994;9(2):133–9.
- [45] Sen Z. Drawdown distribution around a large diameter well with nonlinear groundwater flow. *J Environ Sci Health* 1992;27(7):1817–33.
- [46] Stehfest H. Numerical inversion of Laplace transforms. *Commun ACM* 1970;13(1):47–9.
- [47] Streltsova TD. *Well testing in heterogeneous formations*. New York: Wiley; 1988.
- [48] Van Everdingen AF, Hurst W. The application of the Laplace transformation to flow problems in reservoirs. *Trans AIME* 1949;186:305–24.
- [49] Wilkinson D, Hammond PS. A perturbation method for mixed boundary value-problems in pressure transient testing. *Transp Porous Media* 1990;5(6):609–36.
- [50] Zhan H. Analytical study of capture time to a horizontal well. *J Hydrol* 1999;217:46–54.
- [51] Zhan H, Cao J. Analytical and semi-analytical solutions of horizontal well capture times under no-flow and constant-head boundaries. *Adv Water Resour* 2000;23:835–48.
- [52] Zhan H, Wang LV, Park E. On the interpretation of horizontal-well pumping tests in anisotropic confined aquifers. *J Hydrol* 2001;252:37–50.